Published in final edited form as:
J Immunol. 2014 June 15; 192(12): 5561–5570. doi:10.4049/jimmunol.1400385.

Myeloid Glycosylation Defects Lead to Spontaneous a CVID-Like Condition with Associated Hemolytic Anemia and Anti-Lymphocyte Autoimmunity

Sean O. Ryan, **Derek W. Abbott**, and **Brian A. Cobb**
Case Western Reserve University School of Medicine, Department of Pathology, 10900 Euclid Avenue, Cleveland, OH 44106

Abstract

Common variable immunodeficiency (CVID), the most frequent symptomatic primary immune deficiency in humans, is a heterogeneous group of immunologic disorders estimated to affect 1:10,000 – 1:50,000. Although a clear disease etiology remains elusive, a common characteristic of CVID is deficient IgG antibody production in response to infection or vaccination. Patients often also exhibit autoimmune cytopenias with symptoms of abnormal T cell function, including reductions in naïve T cells which correlate with clinical severity. Here, we discovered that targeted alterations in the glycome of the myeloid lineage lead to spontaneous immunodeficiency characteristic of both humoral and T cell dysfunction regularly found in human CVID. Mice carrying a myeloid-specific knockout of the *Mgat2* gene encoding UDP-GlcNAc:α-6-D-mannoside β-1,2-*N*-acetylglucosaminyltransferase II enzyme exhibit deficiencies in IgG responses to both protein and polysaccharide conjugate vaccines. Interestingly, the immunodeficiency is associated with decreased T cell activity due to a persistent autoimmune-mediated depletion of naïve T cells, which is induced by changes in erythrocyte surface glycosylation. The N-glycosylation dependent auto-epitopes that emerge on erythrocytes lead to autoimmune hemolytic anemia, and the causative auto-IgM cross-reacts with naïve T cells despite the lack of glycan change on T cells. These findings demonstrate that alterations in erythrocyte glycosylation trigger the development of autoantibodies directed at both erythrocytes and naïve T cells, revealing a possible mechanistic link between the induction of autoimmune hemolytic anemia, the reduction in naïve T cells, and poor antibody responses to vaccine in severe CVID patients.

Introduction

CVID is the most commonly diagnosed primary immunodeficiency (1,2), likely due to the variety of clinical presentations, although more than 90% of analyzed CVID patients lack a definitive genetic defect (2). A key characteristic of CVID is poor antibody production, especially IgG, in response to infection or immunization; however, many patients also exhibit symptoms of abnormal T cell function and immune dysregulation (3). The multifaceted nature of this disease coupled with the lack of solid genetics has led to a dearth of available mouse models to understand the manifestations and mechanisms underlying

Correspondence: Brian A. Cobb, CWRU School of Medicine, Dept. of Pathology, 10900 Euclid Avenue, WRB 6532, Cleveland, OH 44106-7288, ph. 216-368-1263, fx. 216-368-0494, brian.cobb@case.edu.

CVID (4). Moreover, the use of Ig replacement therapy (i.e. IVIg) and antibiotics has reduced the number of infections, yet the major inflammatory complications such as autoimmunity still develop in CVID patients (5). As a result, the deficient Ig production common to CVID may not encompass the full mechanistic extent of the disorder.

A broader explanation may be found in multiple observations in which T cell defects were found in a still undefined proportion of human CVID patients. Some CVID patients have significantly decreased T cell numbers, in particular naïve $CD4^+$ T cells (6,7). In a recent clinical study of 313 CVID subjects, patients who developed recurring infections but not autoimmunity showed modest decreases in both class switched memory B cells and naïve $CD4^+$ T cells, while patients with more severe sequelae such as chronic enteropathy showed a greater loss of these cells (8). These studies reveal that the degree of reduction in naïve $CD4^+$ T cells is correlated with clinical disease severity, and that this is independent of age, gender, and even Ig titer (7,8). To date, the mechanisms underlying naïve T cell deficiency have not been identified, though some have postulated that decreased thymic output could account for the changes (7).

In the CVID patient population, autoimmune diseases affect approximately 20% of patients and are commonly the first clinical sign of immunodeficiency (9). Among the various cytopenias, autoimmune hemolytic anemia (AIHA) and autoimmune thrombocytopenic purpura (ITP) are the most prevalent in CVID patients (10). Although the linkage between CVID and these antibody-mediated disorders remains a matter of investigation, it is particularly interesting to note that CVID-associated cytopenia is inversely proportional to the number of naïve $CD4^+$ T cells in circulation, raising the possibility that the specific loss of naïve T cells is mechanistically tied to the destruction of platelets and/or erythrocytes.

We recently described the creation of a novel mouse strain in which we used the cre-lox recombination system to delete the *Mgat2* gene encoding UDP-GlcNAc:α-6-D-mannoside β-1,2-*N*-acetylglucosaminyltransferase II (GlcNAcT-II) within the myeloid lineage (11). These $Mgat2^{\Delta M/\Delta M}$ mice lack the ability to synthesize complex-type N-glycans (cN-glycans) in myeloid cells and are hyporesponsive to T cell-dependent bacterial polysaccharide antigens due to defects in MHC class II-dependent presentation, although peptide responses remain normal and most of these mice do not show overt developmental or systemic defects. However, approximately 25% of these mice show a spontaneous and specific loss of $CD4^+$ naïve T cells despite the lack of change in T cell glycosylation.

Here, we describe the characterization of these spontaneous T cell-depleted $Mgat2^{\Delta M/\Delta M}$ mice to reveal a CVID-like condition that incorporates not only the associated humoral response deficiencies seen in human patients, but also the presence of AIHA coupled with the selective loss of naïve T cells. Our data show that loss of naïve T cells is independent of thymic development or cell-intrinsic *Mgat2* activity, but is associated with significant auto-antibody (IgM) deposition on T cells in circulation, indicating an antibody-mediated mechanism of cell depletion. Remarkably, we found that auto-IgM antibodies arise in response to erythrocytes with altered glycosylation, yet cross-react with naïve T cells from both $Mgat2^{\Delta M/\Delta M}$ and wild type mice. The CVID-like phenotype could also be induced within the 'normal' $Mgat2^{\Delta M/\Delta M}$ mice upon the adoptive transfer of glycan-altered

erythrocytes. These findings demonstrate that changes in erythrocyte glycosylation can trigger IgM-mediated autoimmunity that not only leads to hemolytic anemia, but also cross-reacts with naïve T cells, thereby depleting the helper capacity of the adaptive immune response and preventing robust IgG responses and class switching upon vaccination. Through incorporation of hypogammaglobulinemia, loss of naïve T cells, and AIHA, our findings raise the possibility that altered erythrocyte and/or platelet glycosylation may play an unexpected role in human CVID severity.

Materials and Methods

Animals and common reagents

Animal colonies were maintained in a specific pathogen-free environment at Case Western Reserve University and were treated under IACUC-approved guidelines in accordance with approved protocols. Mgat2$^{\Delta M/\Delta M}$ mice were generated by crossing the Mgat2 (B6.129-*Mgat2*^{tm1Jxm}/J; stock 006892) and LyzM-Cre (B6.129P2-*Lyz2*$^{tm1(cre)Ifo}$/J; stock 004781) parental strains. As reported by Jackson Labs the parental strains were backcrossed to C57BL/6 before inbreeding for nine generations (Mgat2) and at least six generations (LyzM-Cre), respectively. The Mgat2$^{wt/wt}$ mice used were either B6.129-*Mgat2*^{tm1Jxm}/J mice or C57BL/6J mice (stock 000664), both of which have wild type *Mgat2* activity. All mice were originally purchased from Jackson Laboratory. Mouse genotypes were confirmed using Jackson Laboratory PCR protocols. Cell culture was performed using RPMI 1640 media supplemented with 10% FBS, penicillin, streptomycin, L-glutamine, and β-mercaptoethanol (Gibco).

Vaccinations

For protein vaccinations each mouse received an intraperitoneal injection of 2 μg ovalbumin (Sigma) adsorbed to 25 μl alum adjuvant (Alhydrogel® 2%; InvivoGen) in a final volume of 100 μl, diluted in PBS. For polysaccharide vaccinations each mouse received an intraperitoneal injection of 40 μl Prevnar-13® (kindly supplied by John Schreiber, Tufts University, Boston, MA) diluted to 200 μl in PBS. Mice received a second dose at two weeks. Prevnar-13® contains 4.4 μg/ml polysaccharide each from *Streptococcus pneumoniae* serotypes 1, 3, 4, 5, 6A, 7F, 9V, 14, 18C, 19A, 19F, 23F and 8.8 μg/ml from serotype 6B. Mice were analyzed 10 days after the final dose.

Serum antibody detection

Anti-protein and anti-polysaccharide serum antibodies were detected by indirect ELISA as described previously (12,13). Briefly, Microlon high binding plates (Greiner Bio-One) were coated overnight at 4°C with either 10 ug/ml ovalbumin (Sigma) or *S. pneumoniae* serotype 14 polysaccharide (kindly supplied by John Schreiber, Tufts University, Boston, MA) diluted in PBS. Serial dilutions of serum were used to probe antigen bound plates. Detection was performed using biotinylated anti-mouse IgG polyclonal antibody (Jackson ImmunoLabs) and europium-conjugated streptavidin (PerkinElmer) followed by quantification by time-resolved fluorescence on a Victor3V Multilabel Counter using DELFIA Enhancement Solution according to the manufacturer's protocol (PerkinElmer).

Flow cytometry

Flow cytometry was performed as described previously (11). Briefly, cells were stained with AlexaFluor647-conjugated *Phaseolus vulgaris* leucoagglutinin (PHA-L) lectin (Life Technologies) and/or the indicated antibodies (BioLegend) for 30 min at 4°C. FACS data was collected using an Accuri C6 flow cytometer (BD Biosciences). Analyses of FACS data were performed using FCS Express (De Novo Software).

In vitro T cell antigen recall assay

T cell recall assays were performed as described previously (14). $CD4^+$ T cells were isolated from the spleen by $CD4^+$ magnetic bead positive selection (Miltenyi Biotec) and labeled with 2.5 μM carboxyfluorescein diacetate succinimidyl ester (CFSE; Life Technologies). $CD4^+$ T cells (1×10^5) were co-cultured with T cell depleted splenocytes (1×10^5) and 50 μg/ml ovalbumin (Sigma) or media alone. On day 3, culture supernatants were analyzed for IL-5 by sandwich ELISA according to the manufacturer's protocol (BioLegend). To measure proliferation, CFSE-labeled cells were collected and analyzed by flow cytometry.

Coombs test for autoantibody detection

For direct Coombs tests, cells were collected from blood or spleen and probed directly with biotinylated anti-mouse IgM (Jackson ImmunoResearch) and the indicated phenotype antibodies for 30 min at 4°C. For indirect Coombs tests, cells were first incubated at 4°C for 2 hrs with the indicated mouse serum diluted 1:30 in PBS before being probed with biotinylated anti-mouse IgM and the indicated phenotype antibodies. Cells were then washed and probed with AlexaFluor-488 conjugated streptavidin (Jackson ImmunoResearch) followed by analysis by flow cytometry.

Tissue histology and blood differentials

Whole spleens were collected from indicated mice and preserved in 10% buffered formalin (Fisher Scientific). Paraffin embedding, tissue sectioning, and Perls' Prussian blue iron staining were performed by the Tissue Resources Core Facility of the Case Comprehensive Cancer Center (Cleveland, OH). Microscopy images were acquired using a Leica DM IL LED microscope and LAS V4.1 software (Leica Microsystems). Hematological differentials were performed using a HEMAVET analyzer (Drew Scientific).

Complement-mediated lysis assay

Complement lysis assays used Low-Tox®-M rabbit complement (Cedarlane Labs) following the manufacturer's instructions. Blood containing PHA-L^- erythrocytes was collected from naïve $Mgat2^{\Delta M/\Delta M}$ mice into an equal volume of 2 mg/ml EDTA in PBS, pH 7.2. Following three washes with PBS at 1,500 × *g* erythrocyte numbers were determined. 10×10^6 erythrocytes were incubated at 4°C for 2 hrs in 50 μl of the indicated mouse serum diluted 1:30 in PBS. After two washes with PBS, erythrocytes were suspended in 50 μl assay buffer (RPMI with 25 mM HEPES and 0.3% BSA). To each well an additional 50 ul was added of either assay buffer, 1:10 complement diluted in assay buffer, or water. After 1 hr incubation at 37°C intact erythrocytes were removed by centrifugation. Hemolysis was quantified by

measuring supernatant absorbance at 405 nm to determine levels of hemoglobin release. Percent lysis was calculated relative to the water and buffer alone controls.

Adoptive transfer

Cell labeling and adoptive cell transfer experiments were done as previously described (15). Briefly, splenocytes collected from donor Mgat2$^{wt/wt}$ mice were labeled with 6 μM CFSE (Life Technologies) and transferred i.v. at 20×10^6 per recipient Mgat2$^{wt/wt}$ mice or CVID-Mgat2$^{\Delta M/\Delta M}$ mice. On Day 4, spleens from recipient mice were analyzed by flow cytometry to determine absolute numbers of donor cells based on CFSE fluorescence.

Serum antibody adsorption assay

Serum collected from the indicated mice was incubated with erythrocytes from naïve Mgat2$^{\Delta M/\Delta M}$ mice that lack the CVID-like phenotype for 2 hrs on ice in order to adsorb auto-IgM antibodies. This pre-adsorbed serum was collected and incubated with freshly isolated Mgat2$^{wt/wt}$ T cells for 2 hrs on ice, or fresh Mgat2$^{\Delta M/\Delta M}$ erythrocytes to confirm complete auto-IgM removal. Cells were then collected and surface bound IgM was detected using biotinylated anti-mouse IgM and AlexaFluor-488 conjugated streptavidin. T cells were labeled with anti-CD4 and anti-CD44 antibodies. Cells were then analyzed by flow cytometry.

Erythrocyte immunizations

Blood containing PHA-L$^-$ erythrocytes was collected from naïve Mgat2$^{\Delta M/\Delta M}$ mice into an equal volume of 2 mg/ml EDTA in PBS, pH 7.2. Following three washes with PBS at 1,500 × *g* erythrocyte numbers were determined and then subjected to hypotonic lysis using cold buffer containing 5 mM Na_2PO_4 and 1 mM EDTA, pH 8.0. Membranes were washed approximately five times with lysis buffer at 14,000 × g or until residual hemoglobin was not detected in the supernatant as determined by absorbance at 405 nm. Membrane preparations were suspended at 2.5×10^8 input erythrocytes per ml PBS. Each mouse received 200 μl membrane preparation adsorbed to 100 μl alum adjuvant (Alhydrogel® 2%; InvivoGen) by intraperitoneal injection followed by a second injection at two weeks. Mice were analyzed five days after the final injection.

Statistics

Statistical comparisons were performed using a Student's t-test or ANOVA for significance with a 95% confidence interval using GraphPad Instat software. A *p* value less than 0.05 was considered significant.

Results

Myeloid-associated deletion of *Mgat2* induces a hypogammaglobulin state

During our routine characterization of the novel Mgat2$^{\Delta M/\Delta M}$ mouse line, described recently (11), we examined humoral and cellular immune responses induced by vaccination. Mgat2$^{\Delta M/\Delta M}$ mice or Mgat2$^{wt/wt}$ mice were primed with alum-adsorbed ovalbumin. Although a majority of the Mgat2$^{\Delta M/\Delta M}$ responded normally, a population of these mice

was severely IgG hyporesponsive as compared to both Mgat2$^{wt/wt}$ and most Mgat2$^{\Delta M/\Delta M}$ littermates (Fig. 1A). Using the antibody response to segregate Mgat2$^{\Delta M/\Delta M}$ mice into normal and low IgG groups, we could not detect induction of antigen-specific CD4^{+} T cell recall responses, measured by cell proliferation (Fig. 1B) and cytokine production (Fig. 1C), in low IgG Mgat2$^{\Delta M/\Delta M}$ mice as compared to normal IgG Mgat2$^{\Delta M/\Delta M}$ and Mgat2$^{wt/wt}$ mice.

A retrospective analysis of data collected pre-vaccination showed a clear correlation between abnormal CD4^{+} T cell distribution in the blood and vaccine failure. Both Mgat2$^{wt/wt}$ and normal IgG Mgat2$^{\Delta M/\Delta M}$ mice exhibited a “naïve” phenotype pre-vaccination, where CD4^{+} T cells expressing the naïve CD44^{low} surface phenotype were on average at a >10:1 ratio to T cells expressing the effector/memory CD44^{hi} surface phenotype (Fig. 1D). However, low IgG Mgat2$^{\Delta M/\Delta M}$ mice exhibited a significantly skewed <1:1 ratio (Fig. 1D), indicating that a spontaneous pre-existing condition had developed in these mice prior to immunization.

The combination of IgG hyporesponsiveness and T cell dysfunction are characteristics of CVID in humans, with the latter showing a strong association with disease severity (7). Since a common diagnostic of CVID patients is hyporesponsiveness to polysaccharide conjugate vaccines, we further tested our hypothesis that Mgat2$^{\Delta M/\Delta M}$ mice develop a spontaneous CVID-like condition by examining responses to the clinically used Prevnar-13 vaccine. Prevnar-13 is a thirteen-valent capsular polysaccharide conjugate vaccine designed to induce protective antibody-mediated immunity against pneumococcal infection (16). Mgat2$^{\Delta M/\Delta M}$ mice predicted to have the potential CVID-like condition (CVID-Mgat2$^{\Delta M/\Delta M}$) were identified pre-vaccination based on a skewed T cell phenotype in the blood as shown in Figure 1D. As in non-vaccinated mice, humoral IgG responses were undetectable after Prevnar-13 vaccination in CVID-Mgat2$^{\Delta M/\Delta M}$ mice, while responses in “naïve” Mgat2$^{\Delta M/\Delta M}$ mice were induced to a similar extent as control Mgat2$^{wt/wt}$ mice (Fig. 1E).

The abnormal T cell phenotype in CVID-Mgat2$^{\Delta M/\Delta M}$ mice is maintained with age and independent of changes in T cell surface glycosylation

Using the distinct T cell distribution in the blood to identify CVID-Mgat2$^{\Delta M/\Delta M}$ mice, we determined disease penetrance to be approximately 25% of all Mgat2$^{\Delta M/\Delta M}$ mice (Table I). In addition, we found that the phenotype was maintained with age without any detectable conversion between the naïve and CVID-like phenotype (Fig. 2A).

We next examined whether the *Mgat2* conditional deletion was unexpectedly modifying T cells from Mgat2$^{\Delta M/\Delta M}$ mice and thus contributing to the spontaneous immune phenotype. Cell surface labeling with the lectin PHA-L, which preferentially binds cN-glycans and thus can differentiate cells lacking *Mgat2* (11,14), showed no difference in T cell (CD3^{+}) surface glycosylation (Fig. 2B). Alternatively, neutrophils (Gr1^{+}CD11b^{+}), which are known to actively express lysozyme M and thus the focus of most studies using the LyzM-Cre system, showed the expected decrease in cell surface cN-glycans indicated by decreased PHA-L binding (Fig. 2C).

CVID-Mgat2$^{\Delta M/\Delta M}$ mice exhibit autoimmune hemolytic anemia

In addition to poor IgG responses and a loss of naïve T cells, human CVID is also commonly linked to autoimmune cytopenias. To evaluate this in our model, we performed standard hematological analyses and found that the CVID-Mgat2$^{\Delta M/\Delta M}$ mice were somewhat anemic (Fig. 3A). We had shown previously that the hematological profile of naïve Mgat2$^{\Delta M/\Delta M}$ mice was similar to Mgat2$^{wt/wt}$ mice (11). Upon further analysis of the blood, we found a clear population of circulating erythrocytes which failed to bind PHA-L, indicating the lack of cN-glycans, as compared to the uniformly PHA-L^{+} erythrocytes found in Mgat2$^{wt/wt}$ mice (Fig. 3B). Although lysozyme M expression is not commonly associated with the erythroid lineage, the PHA-L binding pattern indicated the loss of *Mgat2* at some point during cell development.

We found that while PHA-L^{-} erythrocytes are a significant proportion of circulating erythrocytes in naïve Mgat2$^{\Delta M/\Delta M}$ mice, the number of PHA-L^{-} erythrocytes in CVID-Mgat2$^{\Delta M/\Delta M}$ mice was much lower (Fig. 3B). Direct Coombs tests showed that CVID-Mgat2$^{\Delta M/\Delta M}$ mice, but not naïve Mgat2$^{\Delta M/\Delta M}$ littermates, had significantly elevated levels of auto-IgM antibody coating erythrocytes, suggesting an anti-erythrocyte response (Fig. 3C). PHA-L^{+} erythrocytes did not exhibit significant auto-IgM antibody deposition between Mgat2$^{\Delta M/\Delta M}$ groups ($p<0.05$), which were similar to control Mgat2$^{wt/wt}$ erythrocytes (Fig. 3D), but rather it was the PHA-L^{-} erythrocytes in CVID-Mgat2$^{\Delta M/\Delta M}$ mice that were the targets of the auto-reactive antibodies (Fig. 3E). Further analysis found that the auto-antibody was functional and could mediate complement lysis (Fig. 3F). Finally, histological analysis showed increased iron deposition in the splenic red pulp of only CVID-Mgat2$^{\Delta M/\Delta M}$ mice (Fig. 3G), indicating heightened clearance of opsonized erythrocytes by resident macrophages. Taken together, these data demonstrate that the spontaneous CVID-like phenotype is also associated with autoimmune hemolytic anemia, similar to many human patients (17), and that this autoimmunity was directed at erythrocytes carrying altered glycans at the cell surface.

CVID-Mgat2$^{\Delta M/\Delta M}$ mice show selective naïve T cell lymphopenia

Based on the active depletion of erythrocytes from CVID-Mgat2$^{\Delta M/\Delta M}$ mice, we postulated that the skewed T cell phenotype (Fig. 1D) may also be due to cell depletion. Indeed, upon closer examination we found that in CVID-Mgat2$^{\Delta M/\Delta M}$ mice, overall CD4^{+} and CD8^{+} T cell numbers in the blood (Fig. 4A) and spleen (Fig. 4B) were significantly decreased. Like human CVID patients, the observed lymphopenia was focused selectively on the naïve T cell population (CD44^{low}; Fig. 4C,D), whereas effector/memory T cell numbers were similar if not slightly increased (CD44^{hi}; Fig. 4E,F). Based on these data, the skewed T cell phenotype ratio (Fig. 1D) appears to be due at least in part to decreased numbers of naïve T cells.

A possible rationale for decreased naïve T cell numbers in the periphery could be related to decreases in thymic output of new naïve T cells. However, overall thymocyte numbers (Fig. 4G) and the relative distribution of cells in the CD4/CD8 double negative, double positive, and single positive stages of development were normal (Fig. 4H). This indicated that the loss

of naïve T cells was independent of thymic development and suggests that the process is actively occurring in the periphery.

Naïve T cells from CVID-Mgat2$^{\Delta M/\Delta M}$ mice are labeled with auto-IgM

Based on the presentation of autoimmune hemolytic anemia, we next sought to determine if the selective absence of naïve T cells in CVID-Mgat2$^{\Delta M/\Delta M}$ mice was due to an ongoing anti-lymphocyte autoimmune response. We found significant levels of auto-IgM deposition on total CD4$^+$ T cells, but not CD8$^+$ T cells (Fig. 5A). Closer examination of the naïve (CD44^{low}) and effector/memory (CD44^{hi}) T cell subsets show that, as predicted, naïve CD4$^+$ T cells (Fig. 5B), and to a lesser extent naïve CD8$^+$ T cells (Fig. 5B) from CVID-Mgat2$^{\Delta M/\Delta M}$ mice were the targets of the auto-IgM antibody. There was no significant antibody deposition on effector/memory T cells as compared to Mgat2$^{wt/wt}$ mice (Fig. 5C).

Naïve T cell lymphopenia in CVID-Mgat2$^{\Delta M/\Delta M}$ mice is not dependent on T cell genotype

Although there was no indication of *Mgat2* deletion in Mgat2$^{\Delta M/\Delta M}$ T cells (Fig. 2), we wanted to confirm that the loss of naïve T cells was independent of cell-intrinsic changes due to the Mgat2$^{\Delta M/\Delta M}$ genotype and thymic development. To this end, we transferred bulk splenocytes from donor Mgat2$^{wt/wt}$ mice to recipient CVID-Mgat2$^{\Delta M/\Delta M}$ mice or control Mgat2$^{wt/wt}$ mice. Three days after transfer, the total number of donor CD4$^+$ and CD8$^+$ T cells remaining in recipient CVID-Mgat2$^{\Delta M/\Delta M}$ mice were significantly decreased compared to recipient Mgat2$^{wt/wt}$ mice (Fig. 6A). As an internal control, the number of donor CD11b$^+$ splenocytes was also determined (Fig. 6A). These myeloid cells were found at equal levels in both recipient groups indicating that the wild type T cells were being selectively depleted. Interestingly, we found that decreased T cell numbers was again due to a selective depletion of naïve CD4$^+$ and CD8$^+$ T cells, but not the effector/memory T cell populations (Fig. 6B). These findings confirm that the mechanism creating T cell lymphopenia in CVID-Mgat2$^{\Delta M/\Delta M}$ mice is an ongoing autoimmune response against naïve T cells.

The auto-antibody response to naïve T cells shares common epitope(s) with erythrocytes expressing the altered glycophenotype

Since it was clear that the autoimmune hemolytic anemia and anti-naïve T cell autoimmunity were both associated with CVID-Mgat2$^{\Delta M/\Delta M}$ mice, we next examined if there was a potential causal link between both conditions, such as through a common autoimmune epitope. We first pre-adsorbed serum from CVID-Mgat2$^{\Delta M/\Delta M}$ mice using erythrocytes from naïve Mgat2$^{\Delta M/\Delta M}$ mice to remove the anti-erythrocyte autoantibody. As compared to total serum that binds to both PHA-L$^-$ erythrocytes and naïve T cells (Fig. 7A), pre-adsorbed serum lost binding to fresh PHA-L$^-$ erythrocytes (Fig. 7B), as expected. Surprisingly, we also saw a loss of T cell binding when using the pre-adsorbed serum (Fig. 7B), suggesting that the auto-antibodies reacting to PHA-L$^-$ erythrocytes share a common epitope with naïve T cells.

To further support the presence of a shared autoimmune epitope, we examined whether breaking *in vivo* tolerance to PHA-L$^-$ erythrocytes in naïve Mgat2$^{\Delta M/\Delta M}$ mice could induce the CVID-like phenotype. Mice were immunized with membrane preparations of PHA-L$^-$ erythrocytes adsorbed to alum adjuvant or given alum alone. Although fold reactivity was

lower than that seen in spontaneous CVID-Mgat2$^{\Delta M/\Delta M}$ mice, PHA-L^{-} membrane preparations did induce a significant auto-antibody response against endogenous PHA-L^{-} erythrocytes (Fig. 8A), yet did not cross-react with the circulating PHA-L^{+} erythrocytes (Fig. 8B). Further indicating a common epitope shared by PHA-L^{-} erythrocytes and naïve T cells, we found significant induction of auto-antibody deposition on circulating naïve CD4^{+} T cells that correlated with a trend of decreased cell numbers (Fig. 8C). As predicted the numbers of effector/memory CD4^{+} T cells were unchanged after immunization, however we did detect some auto-antibody on these cells (Fig. 8D). Unlike the blood, where naïve T cell numbers only trended lower, we did see a significant reduction in their numbers in the spleen of PHA-L^{-} erythrocyte immunized mice (Fig. 8E). Similar to CVID-Mgat2$^{\Delta M/\Delta M}$ mice, there was no significant change in effector/memory T cell numbers (Fig. 8F). Interestingly, there was an inverse relationship between detection of significant auto-antibody deposition in the blood and significant decreases in naïve T cell numbers found in the spleen, suggesting that the opsonized cells in circulation had yet to be cleared from the system. Taken together, our findings indicate that the spontaneous CVID-like condition is directly linked to an auto-antibody response to naïve T cells that shares common epitope(s) with erythrocytes expressing the altered glycophenotype.

Discussion

CVID is a highly heterogeneous disease that is historically categorized by defects in humoral immunity and B cells, however it is estimated that over 30% of the patients also have decreases in absolute T cell numbers, which is due to a selective loss of naïve T cells (6,18). This phenotype has been suggested to indicate a distinct category of CVID, and it perhaps represents the most clinically relevant due to the strong correlation to disease severity (7). Moreover, it is not uncommon for severe CVID to also correlate with autoimmune cytopenias, such as ITP and AIHA (10). In this study, we found that changes in erythrocyte glycosylation can lead to the unmasking of an auto-epitope shared specifically with naïve but not memory or effector T cells. The auto-specific IgM produced leads to the selective depletion of both erythrocytes (AIHA) and naïve T cells. As a result of the loss of naïve T cells, IgG responses to traditional protein and polysaccharide-conjugate vaccines are highly muted. These findings closely mirror a common cluster of phenotypes present in some patients, suggesting that abnormal erythrocyte glycosylation arising from environmental and/or genetic circumstances may contribute to human CVID onset and severity.

We recently described the creation of the Mgat2$^{\Delta M/\Delta M}$ mouse used in these studies (11). The goal underlying that study was to understand the *in vivo* impact of N-linked glycosylation changes upon the MHC class II-mediated presentation of zwitterionic capsular polysaccharide antigens (glycoantigens) to CD4^{+} T cells by altering glycosylation in professional antigen presenting cells (excluding B cells). As we reported, the mice used in that study were from the ~75% of mice from the colony that did not show the autoimmune phenotype. These mice had distinct defects in MHCII-dependent presentation of glycoantigen but not peptide antigen (11). No other defects were seen in any tissue or blood chemistry measures. In this study, we have focused on the ~25% of the colony that develops spontaneous loss of naïve T cells and anemia.

Although initially unexpected, expression of lysozyme M within myeloid stem cell progenitors has been reported previously (19), providing a rationale for why Mgat2$^{\Delta M/\Delta M}$ mice carry as many as 50% of the circulating erythrocytes with a PHA-L-low phenotype. The change in erythrocyte glycophenotype was not independently sufficient to induce anemia or loss of naïve T cells in every Mgat2$^{\Delta M/\Delta M}$ mouse. This incomplete disease penetrance in Mgat2$^{\Delta M/\Delta M}$ mice suggests that the etiology likely has epigenetic origins driven by the microflora. For example, *IL-10* knockout (IL-10$^{-/-}$) mice are a common model for spontaneous inflammatory bowel disease (IBD); however, disease penetrance is highly sensitive to the local environment. IL-10$^{-/-}$ mice housed in full barrier specific pathogen-free (SPF) facilities tend to show incomplete penetrance and mild disease compared to mice in vivariums without a full barrier (20). Furthermore, we detect very little switched (i.e. induced) IgG in non-manipulated mice (wild type and otherwise). Others have reported serum concentrations of IgG to be approximately 10-times higher (~2–3 mg/ml) (21,22) than we detect (~0.25 mg/ml) (Fig. S1). However, when challenged with a generic microbial stimulus such as heat-killed cecal contents, total IgG levels in wild type control mice were significantly increased over that which was induced in CVID-Mgat2$^{\Delta M/\Delta M}$ mice (Supplemental Fig. S1), and thus like CVID patients, we would expect the CVID-Mgat2$^{\Delta M/\Delta M}$ mice to be more susceptible to infection in a non-SPF-environment. Along with the lack of switched IgG induced by vaccination, we also found low B cell numbers in the spleen (Fig. S1). In contrast, the number of B cells in the blood was similar to control animals (Fig. S1), which is a phenomenon commonly seen in CVID patients. This is intriguing because it presents an interesting dichotomy in the mouse that may be missed in humans where measurements are most often taken from the blood rather than a biopsy from the spleen.

The trigger to become CVID-like or not in Mgat2$^{\Delta M/\Delta M}$ mice appears to occur sometime before 5 weeks of age. If it does not occur at these early developmental time points, the CVID-like phenotype does not appear even after well over a year of age and between cage-mates. Moreover, once developed, we have seen no reversal of the phenotype in any mouse. As such, it appears that the development of the CVID-like condition in these mice includes both genetic susceptibility (loss of functional Mgat2) and an unknown environmental trigger. This is an important point because CVID in humans shows remarkable variability in terms of age of onset, and clear links to specific mutations have been largely elusive (2). Given the fact that there is precedent for human disease to be associated with altered glycosylation patterns, such as CDG-IIa (23), breast and ovarian cancer (24,25), rheumatoid arthritis (26), alcoholic liver disease (27,28), and Crohn’s disease (29), it is reasonable to postulate that altered glycosylation may play a role in a subset of CVID cases.

The glycosylation changes resulting from the lysozyme M-powered loss of *Mgat2* does not impact T cell glycosylation. A number of studies have demonstrated that alterations in T cell glycosylation generate abnormal T cell activities. For example, loss of *Mgat5* has been shown to decrease T cell activation thresholds and enhance susceptibility to autoimmune conditions (30). Furthermore, the *Mgat2* complete knockout mouse exhibits significant lymphopenia, in addition to dysmorphic facial features, spinal scoliosis, seizures, and locomotor deficits (31). In Mgat2$^{\Delta M/\Delta M}$ mice, T cell surface glycosylation is

indistinguishable from wild type controls suggesting that T cell glycosylation is not linked to their selective depletion. In fact, we found that CVID-Mgat2$^{\Delta M/\Delta M}$ mice selectively deplete even adoptively transferred wild type naïve but not effector or memory T cells, confirming this interpretation. These findings show that the auto-specific IgM in CVID-Mgat2$^{\Delta M/\Delta M}$ mice is not triggered by changes in T cell surface phenotype, but rather their depletion is the secondary result of auto-antibody generation against targets elsewhere.

With the exception of human aging, CVID is the only other non-infectious disease that is associated with selective loss of naïve T cells. Some reports point to reduced thymic output, as measured by T cell receptor excision circles (18,32) and surface expression of CD31 (7). Since these biomarkers are known to decrease with age during the well-established process of thymic involution and loss of thymic output (33), a similar decrease in CVID patients compared to healthy controls was assumed to be related to thymic dysfunction, however this was not supported with direct analysis of the thymus (7,18). Although reduced thymic output remains a possibility, our findings revealed indistinguishable numbers of single and double positive T cells in the thymus in these mice, leading to an alternative hypothesis whereby the mechanism for loss of naïve T cells is due to a targeted autoimmune response. In humans, this loss of naïve T cells would include recent thymic emigrants and thus when compared to healthy controls, the aforementioned biomarkers would also be expected to be decreased.

Interestingly, we found that the occurrence of AIHA and naïve T cell auto-immunity was related through an apparent common epitope. We have not seen mice with AIHA that did not also have the selective depletion of naïve T cells, nor did we find mice lacking naïve T cells that did not show AIHA. More importantly, we found that ‘immunization’ of mice with PHA-L-negative erythrocyte ghosts could not only induce auto-reactive IgM, but that this IgM also selectively depleted naïve T cells even if those cells were from wild type mice. Finally, ‘absorbed IgM’ from CVID-Mgat2$^{\Delta M/\Delta M}$ serum using PHA-L-negative erythrocyte ghosts also eliminated IgM deposition on native T cells *in vitro* (indirect Coombs test). These data show that alterations in the surface glycosylation of erythrocytes reveal a cryptic epitope shared between erythrocytes and naïve T cells that lead directly to their collective and selective depletion. Therefore, in addition to CVID, the Mgat2$^{\Delta M/\Delta M}$ mice may also be informative for studies of AIHA.

Finally, once naïve T cells are depleted in CVID-Mgat2$^{\Delta M/\Delta M}$ mice, IgG responses to vaccine are severely attenuated. The overall titer of IgG in these mice prior to immunization is not significantly different, further supporting the notion that the naïve T cells are not lost at birth, but rather requires a potent immune response triggered by the presence of PHA-L-negative erythrocytes. However, once those T cells are lost, IgG responses against a model antigen (OVA) and the human conjugate vaccine Prevnar13® mirror the poor response reported for many human CVID patients, thereby completing the circle between loss of erythrocyte complex N-glycans and the defining characteristic of CVID.

In total, we have found that glycosylation changes in the erythrocyte population could explain the incidence of AIHA, loss of naïve T cells, and failure to mount potent IgG responses in some CVID patients. Although we cannot yet say whether this model

recapitulates the mechanism(s) underlying human disease, our findings open exciting new avenues for the study of human CVID with particular attention paid to changes in glycosylation of key hematopoietic cells as a triggering event and possibly as a biomarker for severity.

Supplementary Material

Refer to Web version on PubMed Central for supplementary material.

Acknowledgments

This work was funded by NIH grants GM082916 and OD004225 (B.A.C.). Tissue histology was performed by the Tissue Resources Core Facility of the Case Comprehensive Cancer Center, which is supported by grant P30 CA43703.

We would like to thank Dr. John Schreiber for supplying conjugate vaccine components and Dr. Alex Huang for assistance with microscopy image acquisition.

Abbreviations

CVID	common variable immunodeficiency
IVIg	intravenous immunoglobulin
GlcNAcT-II	β-1,2-*N*-acetylglucosaminyltransferase II
cN-glycans	complex-type N-glycans
AIHA	autoimmune hemolytic anemia
PHA-L	*Phaseolus vulgaris* leucoagglutinin

Reference List

1. International Union of Immunological Societies. Primary immunodeficiency diseases - Report of an IUIS Scientific Committee. Clin Exp Immunol. 1999; 118:1–28.
2. Salzer U, Warnatz K, Peter HH. Common variable immunodeficiency - an update. Arthritis Research & Therapy. 2012:14.
3. Park JH, Resnick ES, Cunningham-Rundles C. Perspectives on common variable immune deficiency. Ann N Y Acad Sci. 2011; 1246:41–49. [PubMed: 22236429]
4. Lee JJ, Rauter I, Garibyan L, Ozcan E, Sannikova T, Dillon SR, Cruz AC, Siegel RM, Bram R, Jabara H, Geha RS. The murine equivalent of the A181E TACI mutation associated with common variable immunodeficiency severely impairs B-cell function. Blood. 2009; 114:2254–2262. [PubMed: 19605846]
5. Resnick ES, Cunningham-Rundles C. The many faces of the clinical picture of common variable immune deficiency. Curr Opin Allergy Clin Immunol. 2012:12.
6. Bateman EA, Ayers L, Sadler R, Lucas M, Roberts C, Woods A, Packwood K, Burden J, Harrison D, Kaenzig N, Lee M, Chapel HM, Ferry BL. T cell phenotypes in patients with common variable immunodeficiency disorders: associations with clinical phenotypes in comparison with other groups with recurrent infections. Clin Exp Immunol. 2012; 170:202–211. [PubMed: 23039891]
7. Giovannetti A, Pierdominici M, Mazzetta F, Marziali M, Renzi C, Mileo AM, De Felice M, Mora B, Esposito A, Carello R, Pizzuti A, Paggi MG, Paganelli R, Malorni W, Aiuti F. Unravelling the complexity of T cell abnormalities in common variable immunodeficiency. J Immunol. 2007; 178:3932–3943. [PubMed: 17339494]

8. Mouillot G, Carmagnat M, Gérard L, Garnier JL, Fieschi C, Vince N, Karlin L, Viallard JF, Jaussaud R, Boileau J, Donadieu J, Gardembas M, Schleinitz N, Suarez F, Hachulla E, Delavigne K, Morisset M, Jacquot S, Just N, Galicier L, Charron D, Debré P, Oksenhendler E, Rabian C. B-cell and T-cell phenotypes in CVID patients correlate with the clinical phenotype of the disease. J Clin Immunol. 2010; 30:746–755. [PubMed: 20437084]
9. Agarwal S, Cunningham-Rundles C. Autoimmunity in common variable immunodeficiency. Curr Allergy Asthma Rep. 2009; 9:347–352. [PubMed: 19671377]
10. Cunningham-Rundles C. Autoimmune manifestations in common variable immunodeficiency. J Clin Immunol. 2008; 28:S42–S45. [PubMed: 18322785]
11. Ryan SO, Leal SM, Abbott DW, Pearlman E, Cobb BA. Mgat2 ablation in the myeloid lineage leads to defective glycoantigen T cell responses. Glycobiology. 2013; 24:262–271. [PubMed: 24310166]
12. Lai Z, Schreiber JR. Outer membrane protein complex of Meningococcus enhances the antipolysaccharide antibody response to pneumococcal polysaccharide-CRM197 conjugate vaccine. Clin Vaccine Immunol. 2011; 18:724–729. [PubMed: 21450979]
13. Ryan SO, Vlad AM, Islam K, Gariepy J, Finn OJ. Tumor-associated MUC1 glycopeptide epitopes are not subject to self-tolerance and improve responses to MUC1 peptide epitopes in MUC1 transgenic mice. Biol Chem. 2009; 390:611–618. [PubMed: 19426130]
14. Ryan SO, Bonomo JA, Zhao F, Cobb BA. MHCII glycosylation modulates *Bacteroides fragilis* carbohydrate antigen presentation. J Exp Med. 2011; 208:1041–1053. [PubMed: 21502329]
15. Ryan SO, Johnson JL, Cobb BA. Neutrophils confer T cell resistance to myeloid-derived suppressor cell-mediated suppression to promote chronic inflammation. J Immunol. 2013; 190:5037–5047. [PubMed: 23576679]
16. Gruber WC, Scott DA, Emini EA. Development and clinical evaluation of Prevnar 13, a 13-valent pneumococcoccal CRM197 conjugate vaccine. Ann N Y Acad Sci. 2012; 1263:15–26. [PubMed: 22830997]
17. Podjasek JC, Abraham RS. Autoimmune cytopenias in common variable immunodeficiency. Front Immunol. 2012; 3:189. [PubMed: 22837758]
18. Guazzi V, Aiuti F, Mezzaroma I, Mazzetta F, Andolfi G, Mortellaro A, Pierdominici M, Fantini R, Marziali M, Aiuti A. Assessment of thymic output in common variable immunodeficiency patients by evaluation of T cell receptor excision circles. Clin Exp Immunol. 2002; 129:346–353. [PubMed: 12165093]
19. Ye M, Iwasaki H, Laiosa CV, Stadtfeld M, Xie H, Heck S, Clausen B, Akashi K, Graf T. Hematopoietic stem cells expressing the myeloid lysozyme gene retain long-Term, multilineage repopulation potential. Immunity. 2003; 19:689–699. [PubMed: 14614856]
20. Sellon RK, Tonkonogy S, Schultz M, Dieleman LA, Grenther W, Balish E, Rennick DM, Sartor RB. Resident enteric bacteria are necessary for development of spontaneous colitis and immune system activation in interleukin-10-deficient mice. Infect Immun. 1998; 66:5224–5231. [PubMed: 9784526]
21. Haury M, Sundblad A, Grandien A, Barreau C, Coutinho A, Nobrega A. The repertoire of serum IgM in normal mice is largely independent of external antigenic contact. Eur J Immunol. 1997; 27:1557–1563. [PubMed: 9209510]
22. Amaral JF, Foschetti DA, Assis FA, Menezes JS, Vaz NM, Faria AM. Immunoglobulin production is impaired in protein-deprived mice and can be restored by dietary protein supplementation. Braz J Med Biol Res. 2006; 39:1581–1586. [PubMed: 17160267]
23. Jaeken J. Congenital disorders of glycosylation. Ann N Y Acad Sci. 2010; 1214:190–198. [PubMed: 21175687]
24. Saldova R, Royle L, Radcliffe CM, Abd Hamid UM, vans RE, Arnold JN, Banks RE, Hutson R, Harvey DJ, Antrobus R, Petrescu SM, Dwek RA, Rudd PM. Ovarian cancer is associated with changes in glycosylation in both acute-phase proteins and IgG. Glycobiology. 2007; 17:1344–1356. [PubMed: 17884841]
25. Turner GA, Goodarzi MT, Thompson S. Glycosylation of alpha-1-proteinase inhibitor and haptoglobin in ovarian cancer: evidence for two different mechanisms. Glycoconj J. 1995; 12:211–218. [PubMed: 7496134]

26. Thompson S, Dargan E, Griffiths ID, Kelly CA, Turner GA. The glycosylation of haptoglobin in rheumatoid arthritis. Clin Chim Acta. 1993; 220:107–114. [PubMed: 8287554]
27. Gravel P, Walzer C, Aubry C, Balant LP, Yersin B, Hochstrasser DF, Guimon J. New alterations of serum glycoproteins in alcoholic and cirrhotic patients revealed by high resolution two-dimensional gel electrophoresis. Biochem Biophys Res Commun. 1996; 220:78–85. [PubMed: 8602862]
28. Mann AC, Record CO, Self CH, Turner GA. Monosaccharide composition of haptoglobin in liver diseases and alcohol abuse: large changes in glycosylation associated with alcoholic liver disease. Clin Chim Acta. 1994; 227:69–78. [PubMed: 7955423]
29. Goodarzi MT, Turner GA. Reproducible and sensitive determination of charged oligosaccharides from haptoglobin by PNGase F digestion and HPAEC/PAD analysis: glycan composition varies with disease. Glycoconj J. 1998; 15:469–475. [PubMed: 9881748]
30. Demetriou M, Granovsky M, Quaggin S, Dennis JW. Negative regulation of T-cell activation and autoimmunity by Mgat5 N-glycosylation. Nature. 2001; 409:733–739. [PubMed: 11217864]
31. Wang Y, Tan J, Sutton-Smith M, Ditto D, Panico M, Campbell RM, Varki NM, Long JM, Jaeken J, Levinson SR, Wynshaw-Boris A, Morris HR, Le D, Dell A, Schachter H, Marth JD. Modeling human congenital disorder of glycosylation type IIa in the mouse: conservation of asparagine-linked glycan-dependent functions in mammalian physiology and insights into disease pathogenesis. Glycobiology. 2001; 11:1051–1070. [PubMed: 11805078]
32. De Vera MJ, Al-Harthi L, Gewurz AT. Assessing thymopoiesis in patients with common variable immunodeficiency as measured by T-cell receptor excision circles. Ann Allergy Asthma Immunol. 2004; 93:478–484. [PubMed: 15562888]
33. Kimmig S, Przybylski GK, Schmidt CA, Laurisch K, Möwes B, Radbruch A, Thiel A. Two subsets of naive T helper cells with distinct T cell receptor excision circle content in human adult peripheral blood. J Exp Med. 2002; 195:789–794. [PubMed: 11901204]

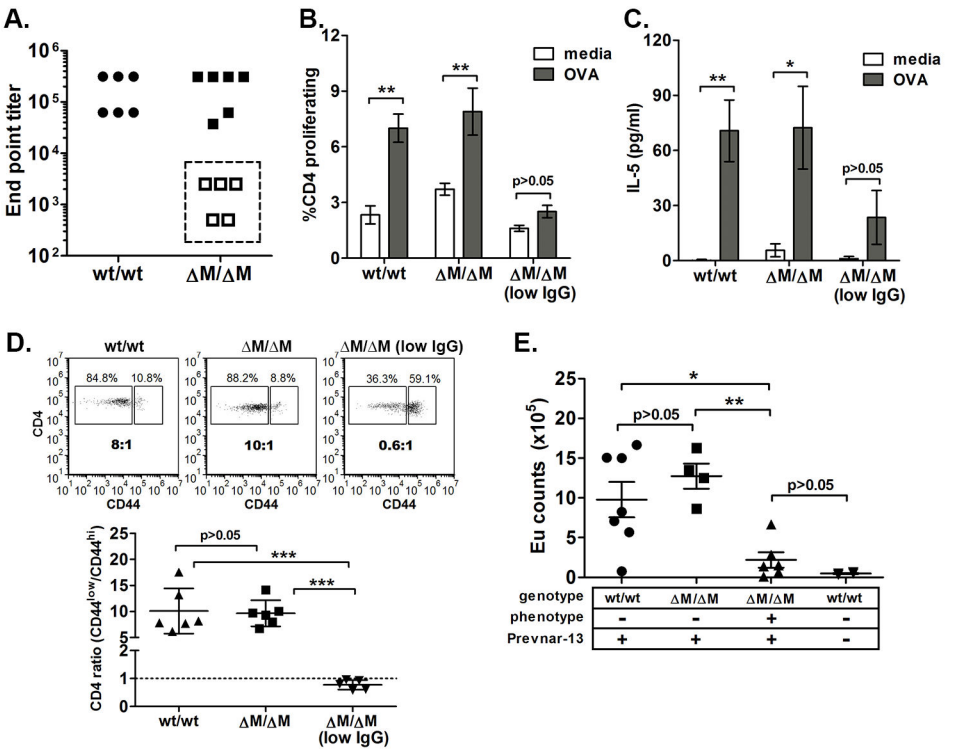

Figure 1. Myeloid-associated deletion of *Mgat2* induces a spontaneous CVID-like condition

$Mgat2^{wt/wt}$ and $Mgat2^{\Delta M/\Delta M}$ mice were immunized with ovalbumin (OVA) and alum. A) Serum anti-ova IgG end point titers identified a sub-set of $Mgat2^{\Delta M/\Delta M}$ mice as low IgG responders (open squares). These low IgG responders did not induce detectable T cell responses to OVA as measured by B) cell proliferation and C) IL-5 production. D) Flow cytometry analysis of blood $CD4^+$ T cells prior to vaccination showing the ratio of naïve ($CD44^{low}$) to effector/memory ($CD44^{hi}$) cells. E) The $CD4^+$ T cell ratio phenotype was used to predict low IgG responders to Prevnar-13 vaccination, show as induced anti-polysaccharide IgG levels by ELISA at 1:50 serum dilution. (Eu, europium) *p<0.05, **p<0.01

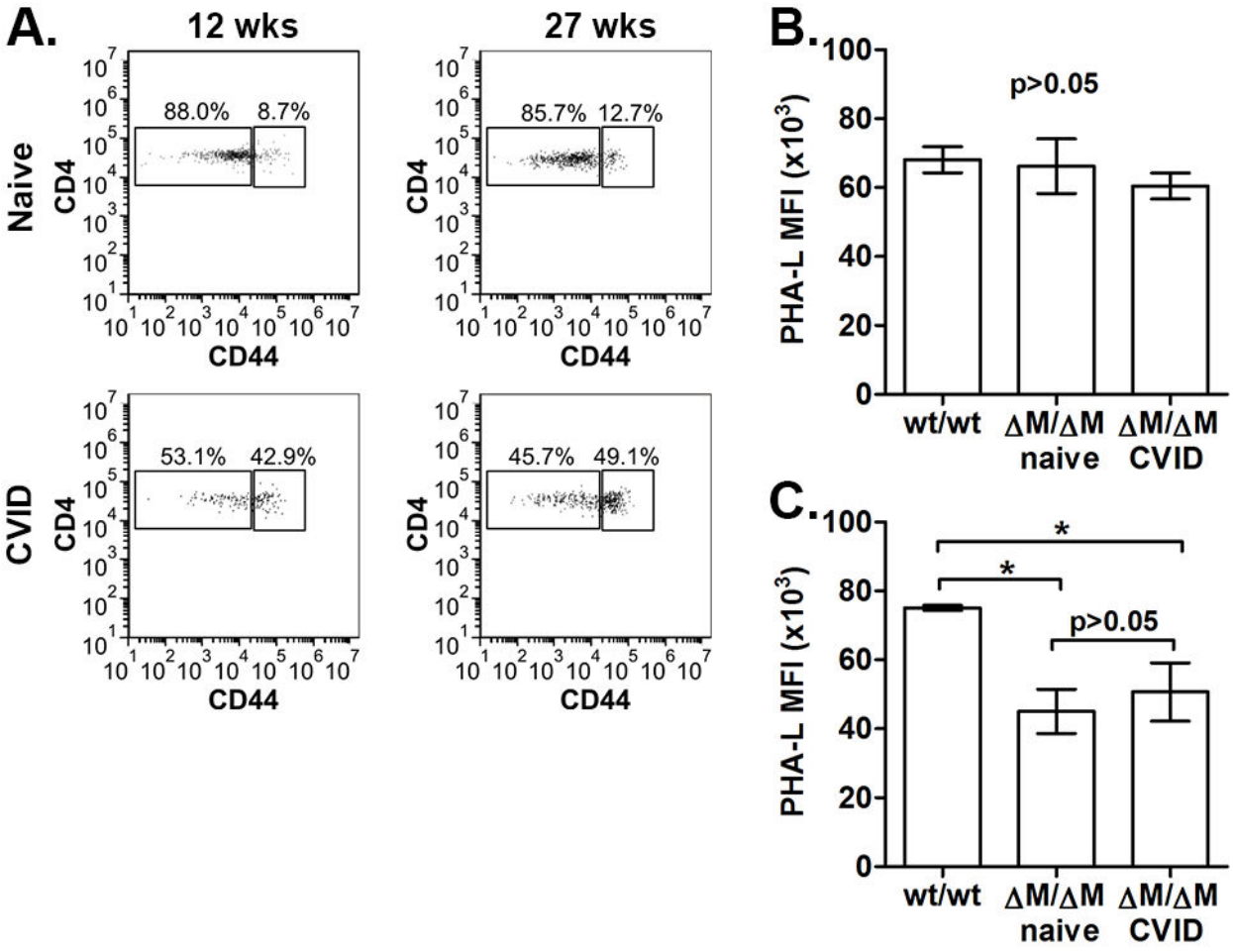

Figure 2. The abnormal T cell distribution in CVID-Mgat2$^{\Delta M/\Delta M}$ mice is maintained with age and independent of changes in T cell surface glycosylation

A) Representative analysis of blood CD4$^+$ T cell phenotype from the same naïve Mgat2$^{\Delta M/\Delta M}$ or CVID-Mgat2$^{\Delta M/\Delta M}$ mouse at 12 and 27 weeks of age. Comparison between B) T cell (CD3$^+$) and C) neutrophil (Gr1$^+$CD11b$^+$) cell glycosylation profiles from Mgat2$^{wt/wt}$, naïve Mgat2$^{\Delta M/\Delta M}$, and CVID-Mgat2$^{\Delta M/\Delta M}$ mice using flow cytometry and fluorescently labeled PHA-L lectin. *p<0.05

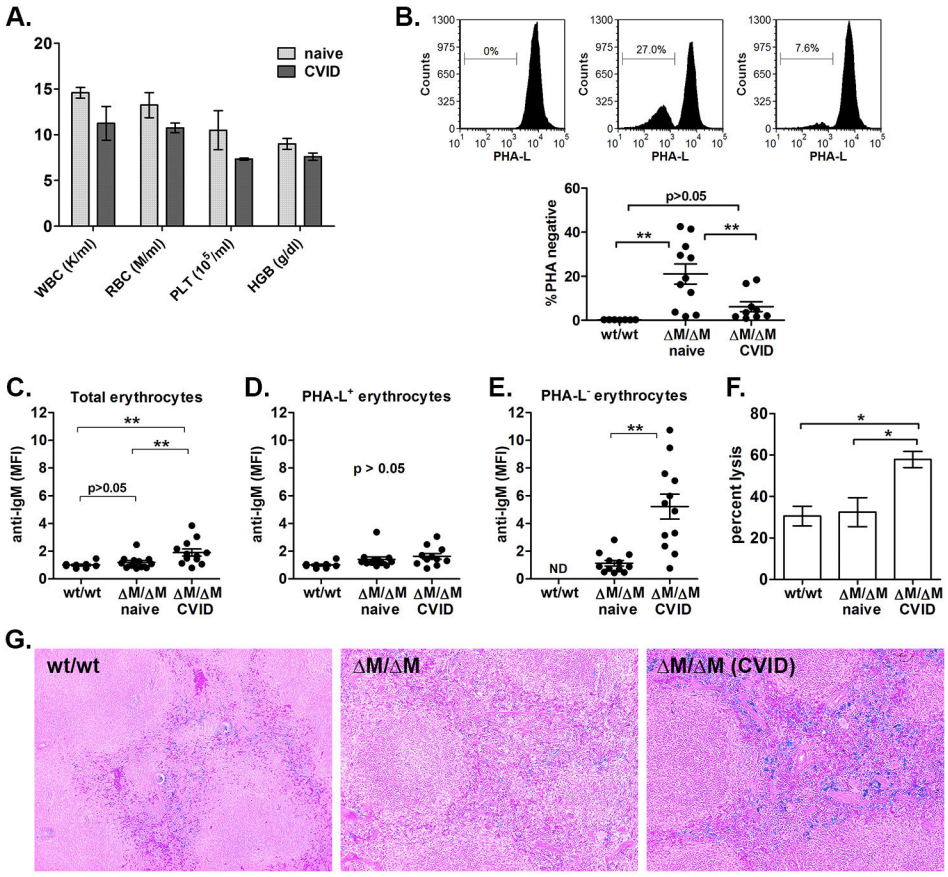

Figure 3. CVID-Mgat2$^{\Delta M/\Delta M}$ mice exhibit a glycophenotype in erythrocytes and CVID-associated autoimmune hemolytic anemia

A) Hematological analysis showing levels of leukocytes (WBC), erythrocytes (RBC), platelets (PLT), and hemoglobin (HGB). B) PHA-L lectin stain of erythrocytes (TER-119^{+}) from Mgat2$^{wt/wt}$ (wt) or naïve and CVID-Mgat2$^{\Delta M/\Delta M}$ mice (n 8). Direct Coombs test was used to identify anti-IgM deposition on C) total erythrocytes and the D) PHA-L^{+} and E) PHA-L^{-} erythrocyte sub-populations. MFI values were normalized to Mgat2$^{wt/wt}$ erythrocytes. PHA-L^{-} erythrocytes were not detected (ND) in Mgat2$^{wt/wt}$ mice. F) Complement-mediated erythrocyte lysis. G) Histological sections were tested for iron deposition using Perls' Prussian blue stain (original magnification 10X). *p<0.05, **p<0.01

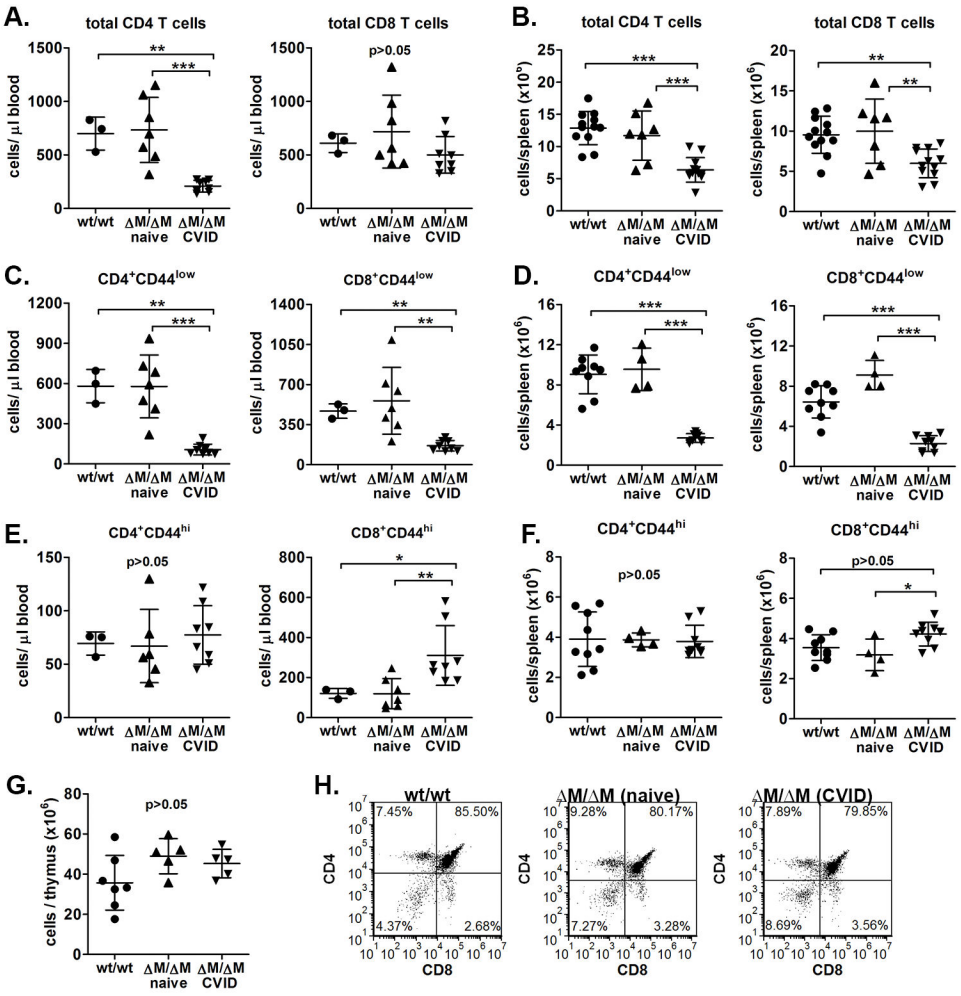

Figure 4. The skewed T cell distribution identifying CVID-Mgat2$^{\Delta M/\Delta M}$ mice is due to selective naïve T cell lymphopenia

Mgat2$^{wt/wt}$ or naïve and CVID-Mgat2$^{\Delta M/\Delta M}$ mice were used to determine total CD4$^+$ and CD8$^+$ T cell counts in A) blood and B) spleen. Naïve (CD44^{low}) CD4$^+$ and CD8$^+$ T cell counts in C) blood and D) spleen. Effector/memory (CD44^{hi}) CD4$^+$ and CD8$^+$ T cell counts E) in blood and F) spleen. G) Total thymocyte counts and H) the stages of thymocyte development based on CD4 and CD8 expression were similar suggesting that loss of naïve T cells is not due to thymic dysfunction in CVID-Mgat2$^{\Delta M/\Delta M}$ mice. *p<0.05, **p<0.01, ***p<0.001

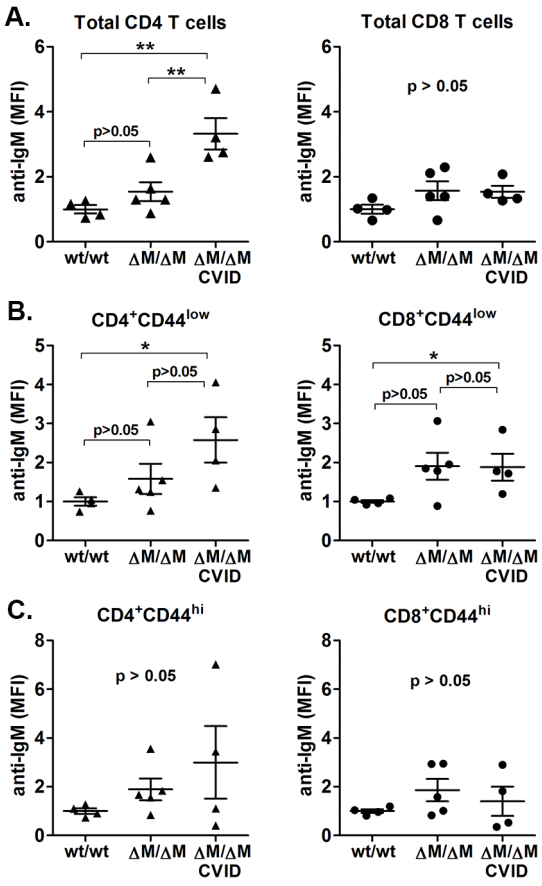

Figure 5. Naïve T cells from CVID-Mgat2$^{\Delta M/\Delta M}$ mice are labeled with auto-IgM antibody

Direct Coombs tests were done to detect auto-IgM adsorbed to A) total CD4$^+$ and CD8$^+$ T cells, B) naïve (CD44^{low}) CD4$^+$ and CD8$^+$ T cells, and C) effector/memory (CD44^{hi}) CD4$^+$ and CD8$^+$ T cells in the blood. *p<0.05, **p<0.01

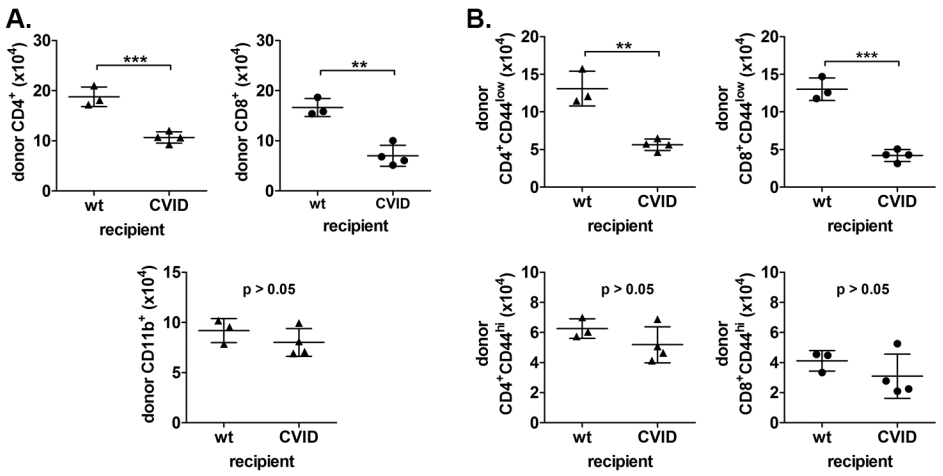

Figure 6. Naïve T cell lymphopenia in CVID-Mgat2$^{\Delta M/\Delta M}$ mice is not dependent on T cell genotype

Donor Mgat2$^{wt/wt}$ splenocytes were labeled with CFSE and transferred into either recipient Mgat2$^{wt/wt}$ mice (wt) or CVID-Mgat2$^{\Delta M/\Delta M}$ mice. After 3 days recipient mice were analyzed to determine the number of remaining donor (CFSE^{+}) A) CD4^{+} and CD8^{+} T cells and CD11b^{+} myeloid cells and B) naïve T cells (top, CD44^{low}) vs. effector/memory T cells (bottom, CD44^{hi}). **p<0.01, ***p<0.001

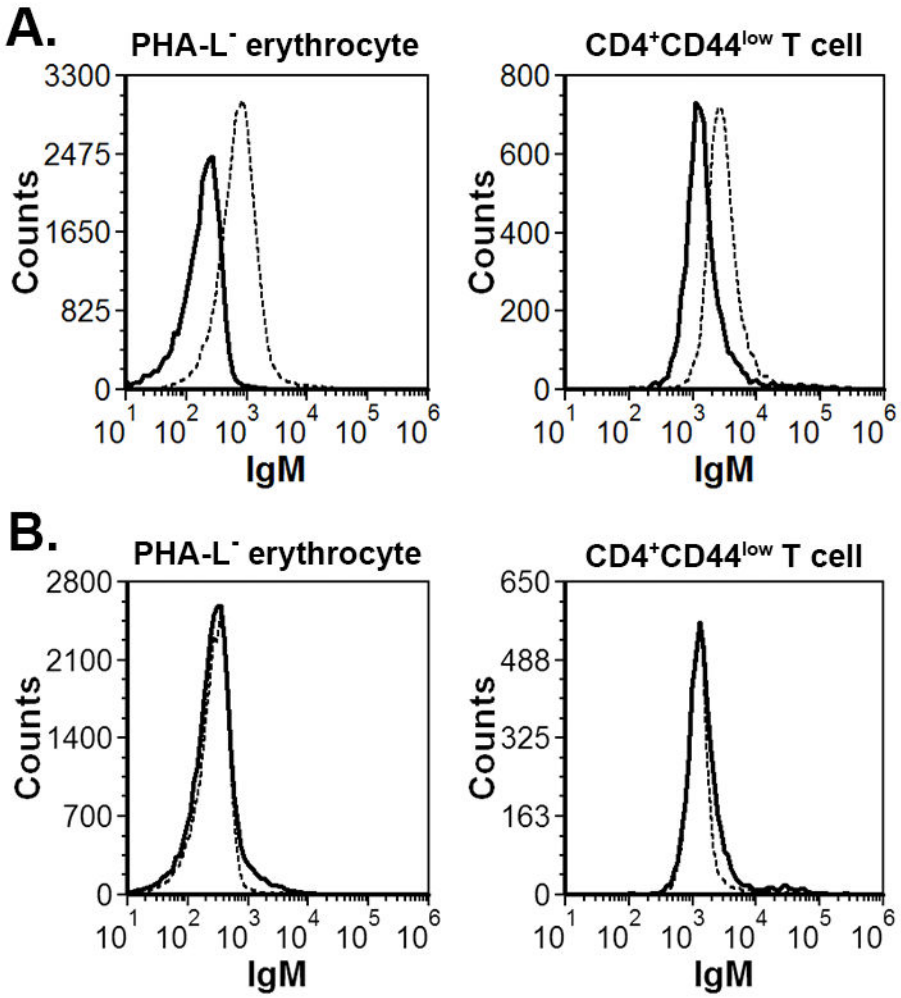

Figure 7. The auto-antibody response to naïve T cells shares common epitope(s) with erythrocytes expressing the altered glycophenotype

Indirect Coombs tests analyzed by flow cytometry showing serum IgM from CVID-Mgat2$^{\Delta M/\Delta M}$ (dashed line) mice, but not Mgat2$^{wt/wt}$ (solid line) mice, binding to PHA-L^{-} erythrocytes and naive CD4^{+}CD44^{low} T cells. B) CVID-Mgat2$^{\Delta M/\Delta M}$ serum (dashed line) and Mgat2$^{wt/wt}$ serum (solid line) was pre-adsorbed to PHA-L^{-} erythrocytes and then used in similar binding experiments with fresh PHA-L^{-} erythrocytes and naive CD4^{+}CD44^{low} T cells. Indicating a common epitope, the adsorption step removed PHA-L^{-} erythrocyte reactivity, as expected, in addition to reactivity to naive CD4^{+}CD44^{low} T cells.

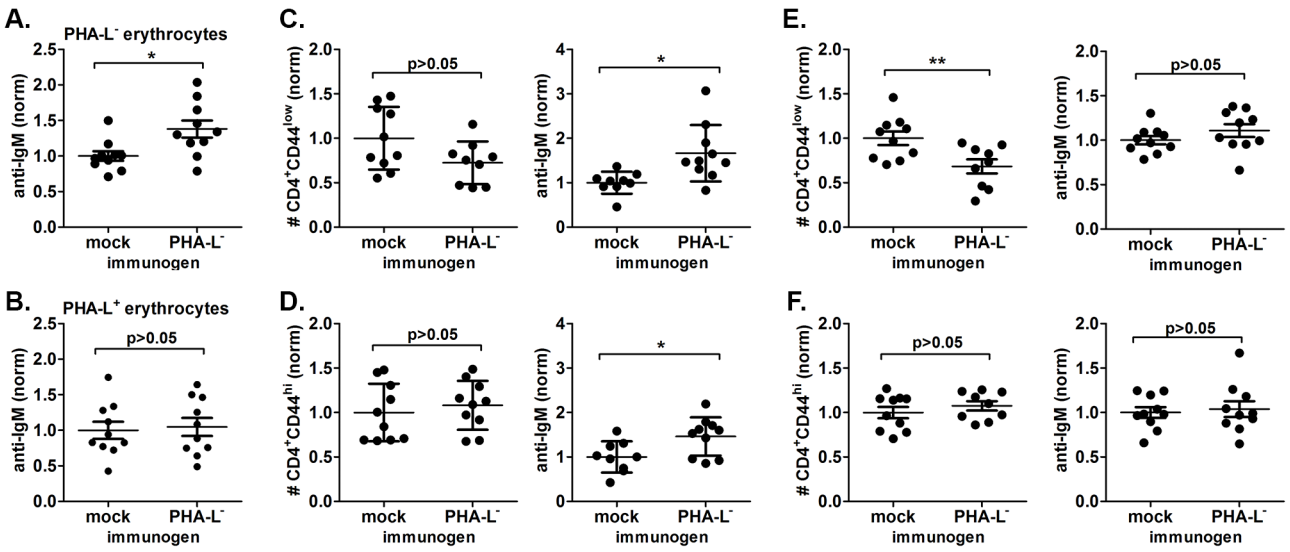

Figure 8. The auto-antibody response to naïve T cells can be induced using erythrocytes expressing the altered glycophenotype

Membrane preparations of PHA-L^{-} erythrocytes were used to immunize naïve Mgat2$^{\Delta M/\Delta M}$ mice. Mice were given three i.p. doses over 4 weeks with alum alone (mock) or alum-adsorbed membranes (immunogen). Direct Coombs tests were performed using flow cytometry to detect induced surface bound auto-IgM to A) endogenous PHA-L^{-} erythrocytes, as compared to B) endogenous PHA-L^{+} erythrocytes. The levels of auto-IgM bound to erythrocytes was normalized (norm) to the average of mock immunized controls. Circulating blood C) naïve CD4^{+}CD44^{low} T cells and D) effector/memory CD4^{+}CD44^{hi} T cells were examined to determine relative cell numbers (left) and level of cell-bound auto-IgM (right). A similar analysis was performed on splenic E) naïve CD4^{+} T cells and F) effector/memory CD4^{+} T cells. Relative T cell numbers and levels of bound auto-IgM were normalized (norm) to the average of mock immunized controls. *p<0.05, **p<0.01

Table I

Incidence of spontaneous CVID-like phenotype

All Mgat2$^{wt/wt}$ mice (n=19) and Mgat2$^{\Delta M/\Delta M}$ mice (n=292) were phenotyped based on CD4 T cell distribution in the blood as shown in Figure 1D.

		Phenotype distribution	
	# naive	# CVID	% CVID
Mgat2$^{wt/wt}$	19	0	0
Mgat2$^{\Delta M/\Delta M}$	218	74	25.3